Effect of constituent particle polydispersion on VSSA-based equivalent particle diameter: Theoretical rationale and application to a set of eight powders with constituent particle median diameters ranging from 9 to 130 nm

Sébastien Bau, Claire Dazon, Olivier Rastoix, Nathalie Bardin-Monnier

Version of Record: https://www.sciencedirect.com/science/article/pii/S092188312100114X
Manuscript_bf3282eafad128f4d14dc853b0082d15

Effect of constituent particle polydispersion on VSSA-based equivalent particle diameter : theoretical rationale and application to a set of eight powders with constituent particle median diameters ranging from 9 to 130 nm

Sébastien Bau*[a], Claire Dazon[b], Olivier Rastoix[a] and Nathalie Bardin-Monnier[c]

a.INRS, Pollutant Metrology Division, F-54519 Vandoeuvre les Nancy, France

b.CEA, Laboratoire des EDifices Nanométriques (LEDNA), F-91191 Gif-sur-Yvette, France

c.Université de Lorraine, Group SAFE, F-54001 Nancy, France

* Email: sebastien.bau@inrs.fr

Abstract

Volume Specific Surface-Area (VSSA) has been identified as a relevant and alternative method to electron microscopy (EM) to determine whether a material is or not a nanomaterial. VSSA is an integral measurement method that provides an indirect representation of particle size. When this conversion into particle diameter is carried out, constituent particles are supposed to be monodisperse, which can be considered far from reality, materials being composed of polydisperse constituent particles. The way particle polydispersion affects the VSSA of a material, and thus the equivalent particle diameter deduced, is investigated in this paper. In particular, the specific case of normally-distributed, spherical constituent particles, is considered. A theoretical study has led to the introduction of a correction polydispersion-based factor. From experimental VSSA data obtained for eight powders covering a range of constituent particle median diameters from 9 to 130 nm, the VSSA-based constituent particle median diameters were compared to the median constituent particle size obtained from electron microscopy analysis, considered as the reference method. Integrating constituent particle polydispersion through the use of the correction factor improves the accuracy of particle size stemming from the VSSA approach, the relative discrepancies being within ± 20% from the reference diameter.

Introduction

Electron microscopy (EM) remains the gold-standard method providing unequivocal information regarding the size distribution of constituent particles, as required in the nanomaterial definition recommendation proposed by the European Commission [1], where the fraction of particles with diameter lower than 100 nm must be determined. However, this

analytical technique, which is expensive and time-consuming, requires a high level of expertise, and lacks of standardized approaches for both sample preparation and particle imaging and analysis, even if some advances can be pointed out on this topic [2]. The issue of analysing sufficient images in order to have a statistically significant analysis [3] is also to be considered, as well as a potential operator effect. Indeed, a coefficient of variation of 6% on the mean particle size was obtained when constituent particle size were measured by three operators from the same TEM pictures of Al_2O_3 [4]. These particles were ideally spherical. In another inter-comparison exercise [5], where each partner was asked to produce its own TEM pictures by means of its own microscope following a common protocol, relative discrepancies of 9% were observed for ERM FD304 SiO_2 sample, which is known for being constituted of spherical constituent particles, and even 15% for a more complex TiO_2 (E171 additive) sample. The same value of 15% was also reported by Dazon *et al.* [6] for spherical particles ranging from 15 to 125 nm.

First introduced by Kreyling *et al.* [7], Volume Specific Surface-Area ($VSSA$) has been identified in the last 10 years as a relevant and alternative method to electron microscopy to determine whether a material is or not a nanomaterial by different authors [8-14], in addition to being mentioned in the definition stemming from the European Commission [1]. It has recently been integrated as tier 1 screening in the NanoDefine as well as the JRC decision trees [15]. $VSSA$ corresponds to the surface-to-volume ratio of a powder material. It is experimentally calculated from the product of the external mass specific surface-area of a powder (SSA), determined through gas adsorption measurements and application of the well-known BET [16] model, and its skeletal density (ρ), measured by Helium pycnometry. It is important to notice that the BET model is no longer valid when the particles are porous. Indeed, for such materials, SSA will correspond to the contribution of both the surface related to the outer dimensions of the constituent particles and the surface due to the presence of pores. In the latter case, specific data processing by using the t-plot model [17] is needed to distinguish between these two contributions to the overall surface area.

According to Dazon *et al.* [8], measuring these two parameters, i.e. SSA and skeletal density, is readily accessible, since the measurement techniques involved are well disseminated in both research laboratories and industries, and can be applied to any type of powders, while electron microscopy is probably less accessible and more subject to operator effects. Furthermore, as stated in Babick *et al.* [11], the advantage of an alternative method based on SSA measurement is that no dispersion protocol is required, which reduces other possible artefacts.

It has been already demonstrated that gas adsorption analysis is relevant and repeatable. Motzkus *et al.* [18] reported relative repeatability standard deviations below 4%, along with relative reproducibility standard deviations lower than 6%, for SiO_2 and TiO_2 nanomaterial powders in the range 50-200 m^2/g investigated in the framework of the Nanogenotox project, except for NM200 (12%). Hackley & Stefaniak [19] compiled the results from 19 laboratories obtained by gas adsorption measurements on a sample of TiO_2 nanomaterial powder; they concluded that the measurement bias was generally within ±5 % of the certified surface area value assigned to SRM 1898 (55.55 ± 0.70 m^2/g). In another study, 9 powders with SSA ranging from 1 to 2.5 m^2/g were also part of an inter-laboratory exercise organized by the National Physical Laboratory involving three partners [20], highlighting SSA mean relative discrepancies of 6%, with a maximum of 12%. Furthermore, due to its quadrupole moment, the orientation of a nitrogen molecule is slightly dependent on the surface chemistry of the adsorbent, which may lead to an uncertainty of about 20% for some surfaces [21, 22]. It is therefore possible to consider that SSA obtained by gas adsorption analysis is accurate within ± 15-20%.

$VSSA$ is an indirect representation of particle size. Indeed, spherical constituent particles of 100 nm with unit density have a $VSSA$ of 60 m^2/cm^3. In line with the seminal proposal made by Kreyling *et al.* [7] and as stated in the definition proposed by the European Commission [1], a non-porous material with a $VSSA$ greater than 60 m^2/cm^3 is a nanomaterial. It has been previously established that this threshold is shape-dependent [9], leading to:

$$VSSA_{cutoff}(\mathrm{m^2/cm^3}) = 20D$$

where $D = 3$ for spheres, $D = 2$ for fibers and $D = 1$ for platelets.

In practice, the VSSA-based equivalent diameter, noted d_{VSSA}, is commonly determined from measured $VSSA$ according to:

$$d_{VSSA}\,(\mathrm{nm}) = \frac{2000D}{VSSA\left(\frac{\mathrm{m^2}}{\mathrm{cm^3}}\right)} = \frac{2000D}{SSA\left(\frac{\mathrm{m^2}}{\mathrm{g}}\right)\rho\left(\frac{\mathrm{g}}{\mathrm{cm^3}}\right)} \quad (1)$$

and compared to the 100 nm threshold. It is important to notice that particle size counts among the parameters which play a key role in the potential health effects of nanoparticles [23], since it defines their deposition probability in the human respiratory tract [24, 25], as well as their behaviour in air [26]. Therefore, deducing the constituent particle size based on an experimental $VSSA$ value can be useful and relevant for instance, in a risk assessment or regulatory context [27], as well as for toxicological studies [28], where the nanomaterial nature of handled powders should be indicated.

Some authors have previously studied the accuracy with which particle diameter can be derived from $VSSA$ measurements. For instance, Babick *et al.* [11] reported that d_{VSSA} deviated from a reference SEM-based particle diameter within a factor 1.5 for 4 out of 9 non-porous materials investigated and a factor 2.5 in the worst case. In the study conducted by Dazon *et al.* [29], relative discrepancies between -3 % and +30 % were reported between SEM-based and VSSA-based particle diameters for the seven non-porous materials investigated. In another study [30], a relative discrepancy of 12% is reported between TEM-based and VSSA-based constituent particle size on a sample of alumina consisting of spherical 25-nm particles.

The discrepancies reported by the different authors highlight the need for investigating the sources of uncertainty that can affect the VSSA-based equivalent d_{VSSA}. Among them, particle shape (D) is probably the key element, since it influences directly the threshold above which a material is classified as a nanomaterial. To our best knowledge, the only way allowing particle shape to be quantified is based on a rigorous examination of EM pictures. Determining precisely whether constituent particles have a spherical, fiber-like or platelet-like morphology remains nonetheless quite difficult in some cases. Another concern can be raised for samples containing particles presenting different morphologies, which could be the case of mixes, for instance rutile (fiber-like particles) and anatase (near-spherical particles) TiO_2 particles. In such cases, an average shape factor might be appropriate to apply equation 1.

The second parameter involved in equation 1 is the skeletal density of the material. The latter can be found in the open literature for pure materials or calculated from published data when the chemical composition and the crystalline phase of the sample is known. Experimental measurement of the skeletal density of powders by pycnometry can be considered accurate. For example, relative discrepancies lower than 1% were reported [31, 32], in line with previous work conducted by Rude *et al.* [33] on fibres.

The last factor of influence is related to the fact that, when equation 1 is applied, constituent particles are supposed to be monodisperse. This strong hypothesis can be considered far from reality, since materials are typically composed of polydisperse constituent particles [2, 27]; the latter being potentially either agglomerated or even aggregated within the material. It is worth mentioning that constituent particle polydispersion influences agglomerate light scattering [34, 35], thermal properties [36-38], behaviour in air [39] including filtration [40, 41], to cite a few.

From a practical point of view, when the SSA of a powder sample is measured by gas adsorption, it is intrinsically accounted that constitutive constituent particles of this sample are polydisperse, since this technique belongs to the so-called “integral measurement

techniques". Indeed, SSA is defined by the total surface area (S) present in a powder sample divided by the mass (M) of this sample:

$$SSA = \frac{S}{M} = \frac{\sum_d S(d)}{\sum_d M(d)}$$

while the result of such analysis does not allow the size distribution of the constituent particles to be determined. This is also the case for Helium pycnometry used to determine powder skeletal density. By extension, the same can be stated for the $VSSA$, since:

$$VSSA = \frac{S}{V} = \rho.SSA = \rho\frac{\sum_d S(d)}{\sum_d M(d)}$$

Therefore, it is important to investigate the way particle polydispersion affects the $VSSA$ of a material, and *in fine* the equivalent particle diameter that is commonly deduced from this parameter. This was indicated by Kreyling *et al.* [7], who state that "one possible way would be to extend the definition such that it uses a second parameter; for instance the standard deviation of a normal distribution, or geometric standard deviation of a lognormal distribution".

For a non-porous spherical particle, particle mass increases faster than its surface-area, and $VSSA$ is therefore inversely proportional to particle diameter:

$$VSSA \sim \frac{1}{d}$$

It is thus manifest that the $VSSA$ of a polydisperse material, typically distributed according to normal or lognormal distribution laws, will be lower than the one of a monodisperse material with the same median diameter (Figure 1). In other words, measuring $VSSA$ lower than the cutoff value does not necessarily indicate that particles are greater than 100 nm. By extension, the VSSA-based equivalent diameter might be falsely overestimated.

To meet these needs, this paper aims at providing elements that can be used to take into account constituent particle polydispersion in order to correct the VSSA-based equivalent diameter. The particular case of normally-distributed, spherical constituent particles, will be considered. Even though this model of distribution law may not be universal, this paper proposes an approach that could be further adapted to any type of distribution.

In a first step, a theoretical development is proposed to formalize the effect of particle polydispersion of VSSA-based equivalent diameter. The findings stemming from this first part will then be applied to a set of eight materials, with constituent particle median diameters ranging from 9 to 130 nm. The results will be compared to the median constituent particle size obtained from transmission electron microscopy (TEM) analysis, considered as the reference method. In the absence of data related to the number size distribution of

constituent particles, an alternative approach based on a hypothesis of constituent particle polydispersion will also be investigated.

Theoretical background

The effect of constituent particle polydispersion on VSSA-based equivalent diameter

The fact that the $VSSA$ of a polydisperse material is lower than the one of a monodisperse material with the same median diameter is illustrated in Figure 1.

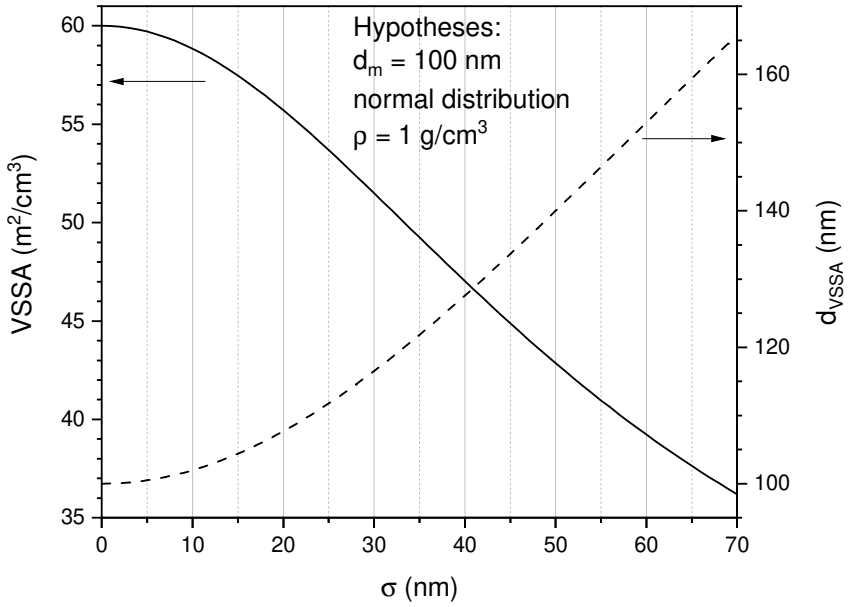

Figure 1. Evolution of the Volume Specific Surface Area ($VSSA$) of a powder with the standard deviation σ of the number size distribution of spherical constituent particles assumed to be normally distributed around a median value of $d_m = 100$ nm (left axis) and the corresponding equivalent diameter d_{VSSA} as calculated from equation 1 (right axis).

In Figure 1, the $VSSA$ of a powder is represented against the standard deviation σ of the number size distribution of its constituent particles (assumed to be spherical and normally distributed) for the case of a median value diameter $d_m = 100$ nm, associated with the corresponding equivalent diameter d_{VSSA} (equation 1).

It is clear from Figure 1 that a powder composed of constituent particles with a median diameter of 100 nm and a standard deviation of 30 nm presents a $VSSA$ of roughly 50 m^2/cm^3, which is 17% lower than the one of a material constituted of monodisperse 100 nm particles (60 m^2/cm^3). In terms of particle equivalent diameter, this $VSSA$ of 50 m^2/cm^3 returns a value of 117 nm equivalent diameter. If this value is the only one available when identifying nanomaterials is sought, e.g. no electron microscopy is envisaged to confirm or

infirm it, it will lead to a false-negative non-nanomaterial. Indeed, in this example, the proportion of particles smaller than 100 nm is 50%, which makes the material fall into the category of nanomaterials according to the European Commission definition.

Modelling the impact of constituent particle polydispersion on VSSA-based equivalent diameter

Let us consider a powder material constituted by agglomerated spherical, non-porous particles (referred to as constituent particles in the remainder of this paper), of diameter d, whose number size distribution follows a mathematical law noted $N(d)$. The $VSSA$ of this powder material is given by the general equation (equation 2) that corresponds to the ratio of the sum of each particle surface-area to the sum of each particle volume:

$$VSSA = \frac{S}{V} = \frac{\int_{d_{min}}^{d_{max}} N(d)\pi d^2 \mathrm{d}d}{\int_{d_{min}}^{d_{max}} N(d)\frac{\pi}{6} d^3 \mathrm{d}d} \quad (2)$$

as stated in the JRC report [42].

For the case of monodisperse constituent particles, with diameter d, the size distribution is assimilated to a Dirac function $N(d) = \delta(d)$ such that $\int_{d_{min}}^{d_{max}} \delta(d)\mathrm{d}d = 1$, and therefore:

$$\int_{d_{min}}^{d_{max}} N(d)\pi d^2 \mathrm{d}d = \pi d^2 \quad (3)$$

$$\int_{d_{min}}^{d_{max}} N(d)\frac{\pi}{6} d^3 \mathrm{d}d = \frac{\pi}{6} d^3 \quad (4)$$

The latter equations 3 and 4 yield the well-known relationship between the Volume Specific Surface-Area of a material and the VSSA-based equivalent diameter of its spherical constituent particles:

$$VSSA_{mono} = \frac{6}{d_{VSSA,mono}} \quad (5)$$

Let us now consider polydisperse constituent particles, and assume that their number size distribution follows a normal distribution:

$$N(d) = \frac{N_{tot}}{\sigma\sqrt{2\pi}} \exp\left[-\frac{1}{2}\left(\frac{d - d_m}{\sigma}\right)^2\right] \quad (6)$$

where d_m represents the median particle diameter and σ the standard deviation. Equation 2 can be written:

$$VSSA_{poly} = \frac{\int_{d_{min}}^{d_{max}} \exp\left[-\frac{1}{2}\left(\frac{d - d_m}{\sigma}\right)^2\right] \pi d^2 \mathrm{d}d}{\int_{d_{min}}^{d_{max}} \exp\left[-\frac{1}{2}\left(\frac{d - d_m}{\sigma}\right)^2\right] \frac{\pi}{6} d^3 \mathrm{d}d} \quad (7)$$

After integration, we obtain (see Appendix):

$$VSSA_{poly} = \frac{6}{d_m} \frac{1 + \left(\frac{\sigma}{d_m}\right)^2}{1 + 3\left(\frac{\sigma}{d_m}\right)^2} \quad (8)$$

Introducing $VSSA_{mono}$ from equation 5 and defining the polydispersion-based factor θ by:

$$\theta = \frac{1 + \left(\frac{\sigma}{d_m}\right)^2}{1 + 3\left(\frac{\sigma}{d_m}\right)^2} \quad (9)$$

yields:

$$VSSA_{poly} = VSSA_{mono}\theta \quad (10)$$

It is worth mentioning that for monodisperse particles, $\sigma = 0$ and consequently $\theta = 1$. Figure 2 presents the evolution of the polydispersion-based factor θ with the ratio σ/d_m for spherical, normally distributed constituent particles.

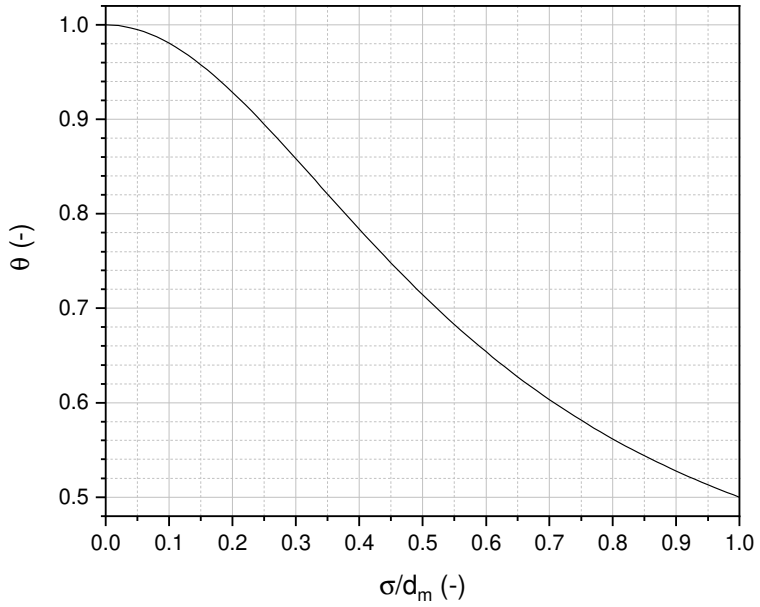

Figure 2. Evolution of the polydispersion-based factor θ with the ratio σ/d_m for spherical, normally distributed constituent particles.

It can be observed from Figure 2 that in the range of σ/d_m between 0 and 1, θ varies between 1 (monodisperse particles) and roughly 0.5. Again, since $\theta \leq 1$, and according to equation 10, the $VSSA_{poly}$ of a powder consisting of polydisperse constituent particles is lower than the one of monodisperse particles with identical median diameter.

Therefore, in terms of VSSA-based equivalent diameter (noted $d_{VSSA,poly}$), equation 10 can be written as:

$$d_{VSSA,poly} = \frac{6\theta}{VSSA_{poly}} \quad (11)$$

Integrating equation 5 leads to:

$$d_{VSSA,poly} = d_{VSSA,mono}\theta \quad (12)$$

Hence, based on equation 12, if the determination (or an hypothesis on) the ratio σ/d_m of the constituent particles composing a powder is available, the factor θ could be used as a correction factor to deduce the VSSA-based equivalent diameter $d_{VSSA,poly}$.

As stated earlier, equation 12 has been established for spherical normally-distributed constituent particles. The same theoretical approach could be followed to investigate different particle shapes (fiber-like or platelet-like particles), as well as other distribution laws. Indeed, some works report that lognormal distributions are more appropriate to describe the size distribution of particles [43-47]. Assuming other mathematical models will impact the expression of the distribution function $N(d)$, and therefore Equation 6. If it cannot be stated that the normal distribution is the most appropriate law, it allows the full mathematical resolution of Equation 7. This specific case shall be considered as an example that could be further examined through the use of other models.

Materials and methods

Eight powders were considered in this study: three titanium dioxides TiO_2, four silicon dioxides SiO_2 and an iron oxide Fe_2O_3. Experimental data were carried out by two research laboratories, named "A" and "B". It is important to notice that the analytical instruments involved by each laboratory were slightly different, as described below. To state on the possible bias between the $VSSA$ data stemming from both laboratories involved, the SSA of TiO_2 3 as well as two SiO_2 samples (SiO_2 1 and SiO_2 3) characterized by lab A was also determined by lab B, yielding relative discrepancies of 10%, 4% and 0.5%, respectively. Samples TiO_2 3 and SiO_2 1 correspond to the lowest and largest SSA, while SiO_2 3 sample has an intermediate SSA (see "Results and Discussion"). These intercomparison data are thus in line with the range of inter-laboratory biases of ± 15-20% stated in the Introduction. Moreover, a similar intercomparison was carried out on the same samples regarding powder density, leading relative discrepancies of 4.6%, -5.7% and 3.0%, respectively.

In spite of different analytical instruments involved, the data can be considered as relevant for further use to determine the VSSA-based equivalent diameter. Therefore, in the remainder of this paper, only one set of data per powder sample will be considered.

Reference particle diameter by electron microscopy

As stated earlier and considering electron microscopy as the reference method, images were used to establish the size distribution of the constituent particles in the powder when the number of identifiable and isolated particles in the acquired images is sufficient [4, 47, 48].

A short theoretical study was conducted to investigate the effect of the number of constituent particles measured on the average size, and finally optimize this number of particles to be measured leading to a satisfying median value. Therefore, we simulated particle sizes distributed according to a normal law. From this simulated dataset, N values were randomly extracted and used to determine the corresponding size distribution. Two extreme conditions were used in the simulations: a realistic case ($\sigma/d_m = 0.4$ – top on Figure 3) and a "best" case ($\sigma/d_m = 0.005$ – bottom on Figure 3). We performed calculations for N = 10 to 500 measurements.

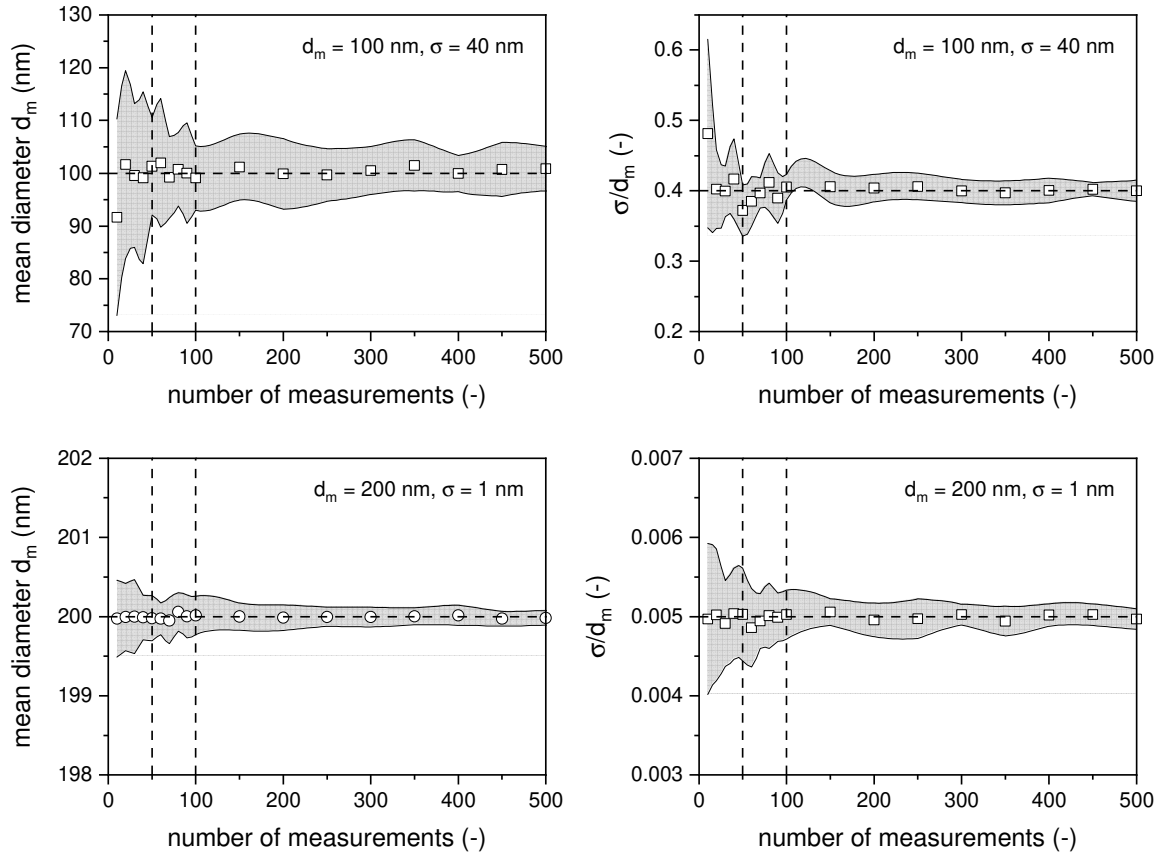

Figure 3. Theoretical study of the effect of the number of particles measured from TEM pictures on the median diameter d_m and the polydispersion σ/d_m. The grey areas correspond to the 95%-confidence interval.

According to Figure 3, determining the average particle size on 50 measurements is acceptable, the bias between theoretical median value and the one from the 50 randomly-generated particles being found below 2%. Determining the average size on 100 measurements does not significantly modify the average size obtained (bias shifts from 1.3% to -0.8% for the realistic case, it even does not change at all (0%) for the best case). For these reasons, determining the constituent particle size distribution on a set of $N \geq 50$ measurements can be considered accurate and reliably used. This cutoff corresponds to the smaller number of particles to be counted as advised by De Temmerman *et al.* [47].

TEM samples were prepared following the specific "grid-on-drop" method [49-51] using TEM copper 400 mesh carbon film grids (Agar Scientific, Essex, England). One grid per powder sample was analysed with a TEM CM 200 (Philips) at 200 kV for samples treated by lab A and with a STEM 2100-F (Jeol) at 200 kV for samples investigated by lab B.

For each powder, between 15 and 20 images were collected at 200 kV with magnifications between ×195 and ×100000. These images were further treated using ImageJ software (U. S. National Institutes of Health, Bethesda, Maryland, USA, https://imagej.nih.gov/ij/, version 1.52). In practice, the projected surface-area A of a constituent particle is measured and converted into diameter d assuming particle sphericity (as stated in Equation 1):

$$d_{TEM} = \sqrt{\frac{4A}{\pi}} \tag{13}$$

In the present study, number size distributions were based on a number of particles counted ranging from 83 to 373, which is in line with the "critical" amount of 50 as mentioned above.

The data provided by TEM-based analysis were then fitted by a normal function, which yields the median particle diameter d_m and the associated standard deviation σ. The fit was performed using Origin Pro software (OriginPro, Version 2019b, OriginLab Corporation, Northampton, MA, USA). For both parameters, the 95%-confidence interval was also determined. As stated earlier, a different model from the normal function could also be implemented, the choice of the model shall be made depending on experimental data.

VSSA-based particle diameter

As already mentioned, the $VSSA$ of a powder corresponds to the product of the external mass specific surface-area of a powder (SSA) and its skeletal density (ρ). In practice, determining these two characteristics involves gas adsorption and Helium pycnometry. As an "integral measurement technique" evoked earlier, both the SSA and skeletal density

measured for a powder sample intrinsically accounts for the polydispersion of its constituent particles. Therefore:

$$VSSA_{measured} = VSSA_{poly} = \rho_{measured}.SSA_{measured}$$

External mass specific surface-area

Nitrogen adsorption was performed with an ASAP 2020 (Micromeritics) for lab A samples, and a Belsorp-Max (Bel Japan) for lab B samples. All the powders were outgassed a minimum of 12 h under vacuum at 200°C before proceeding to N_2 adsorption experiments. Outgassing is necessary to remove from the powder particle surfaces eventually adsorbed water and pollutants molecules which can entail an underestimation of the surface areas measured [22, 52].

All N_2 adsorption measurements were performed at 77 K and triplicated (three samples analysed for each powder). The external mass specific surface areas were determined using the BET model [16], applied in a range of relative pressures from ~ 0.05 to ~ 0.25.

Particle skeletal density

The skeletal densities of the powders were determined by Helium pycnometry (Accupyc 1340, Micromeritics for lab A samples; Belsorp Max, Bel Japan for lab B samples). All the powders were dried overnight in an oven at 150°C before performing the measurements.

Experimental skeletal density measurements were validated by comparison of the results obtained with the theoretical material densities, as stated in Dazon *et al.* [29].

Equivalent particle diameter

The determination of the VSSA-based equivalent particle diameter was first carried out putting aside the polydispersion of constituent particles, according to:

$$d_{VSSA,mono} = \frac{6}{\rho_{measured}.SSA_{measured}} \quad (14)$$

As already mentioned, integrating the polydispersion of constituent particles leads to introducing the polydispersion-based factor θ:

$$d_{VSSA,poly} = \frac{6\theta}{\rho_{measured}.SSA_{measured}} \quad (15)$$

In the latter equation, the VSSA-based equivalent diameter $d_{VSSA,poly}$ is θ-dependent. In most cases, the number size distribution of constituent particles used to determine θ, is unknown because of the absence of electron microscopy analysis. To overcome this issue, an alternative approach considering a polydispersion of $\sigma/d_m = 0.25$ can be investigated (see

Table 2), which yields $\theta = 0.9$ (equation 9). The corresponding VSSA-based equivalent diameter will be noted $d^*_{VSSA,poly}$ in the remainder of this paper.

Results and discussion

Powder textural properties

The eight powders selected cover a wide range of $VSSA$ from 37 to 540 m^2/cm^3 (Table 1). It was verified that gas adsorption isotherms were of either type II or type IV according to IUPAC classification [21], which allowed the BET model to be applied when determining the SSA of the powders [13, 29, 53, 54], and demonstrated the non-porous nature of the particles.

Table 1. Characteristics of the eight powders investigated.

Substance	Lab	SSA (m^2/g)	ρ (g/cm^3)	$VSSA$ (m^2/cm^3)
TiO_2 1	B	141	3.82	538
TiO_2 2	B	11.3	3.96	45
TiO_2 3	A	9.5	3.89	37
SiO_2 1	A	245	2.30	566
SiO_2 2	B	178	1.91	340
SiO_2 3	A	152	2.33	354
SiO_2 4	A	21.3	2.26	48
Fe_2O_3	B	41	4.74	194

TEM-based constituent particle diameter

A typical TEM picture of each of the powders is provided in Figure 4, highlighting nearly-spherical constituent particles. In Figure 4, as well as in the remainder of this paper, the samples are ranked from the smallest to the largest primary particles.

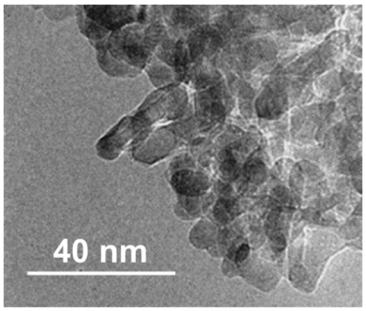

TiO_2 1

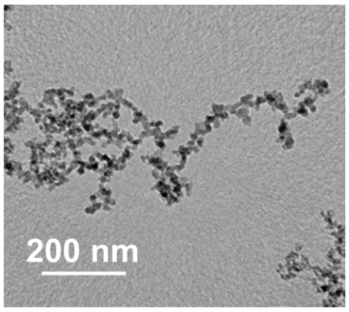

SiO_2 1

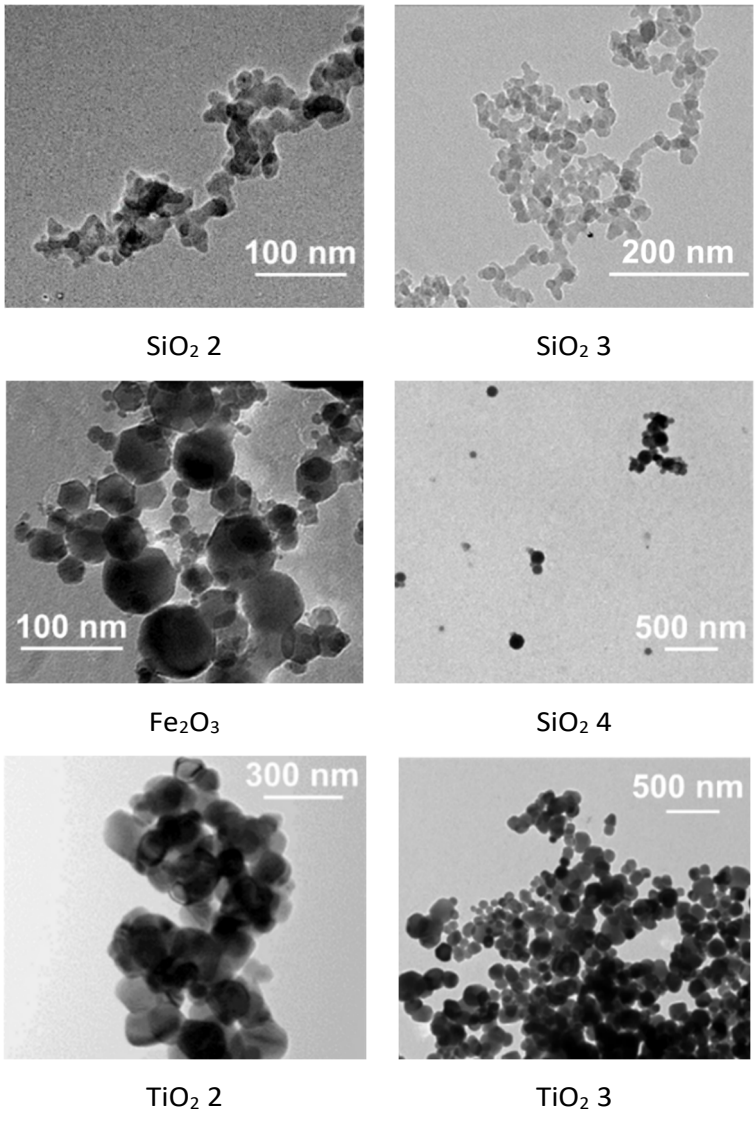

SiO_2 2 SiO_2 3

Fe_2O_3 SiO_2 4

TiO_2 2 TiO_2 3

Figure 4. TEM pictures of each of the powders under study.

It can be observed from Figure 4 that SiO_2 1, 2 and 3 seem to be constituted of aggregated constituent particles, contrary to other materials for which constituent particles appear agglomerated. For TiO_2 1, the shape of the constituent particles is more difficult to define.

The number size distributions of constituent particles determined from TEM analysis are presented in Figure 5, along with the normal fits. The median diameter of the constituent particles was found to cover the particle size between 9 and 130 nm and is therefore supposed to cover a wide range of materials.

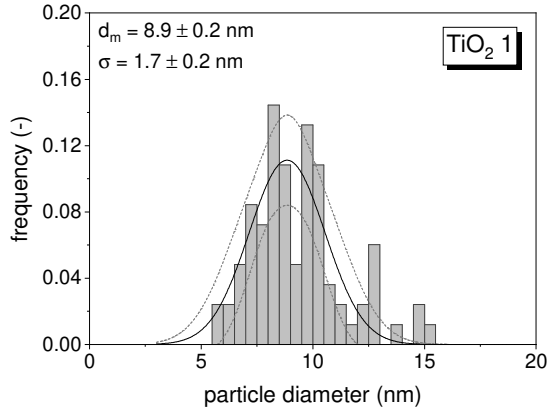
d_m = 8.9 ± 0.2 nm
σ = 1.7 ± 0.2 nm
TiO_2 1
frequency (-)
particle diameter (nm)

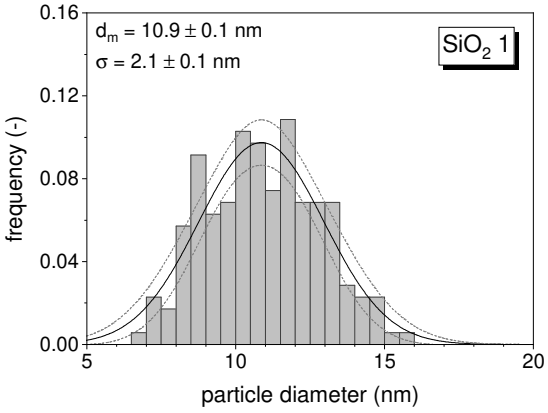
d_m = 10.9 ± 0.1 nm
σ = 2.1 ± 0.1 nm
SiO_2 1
frequency (-)
particle diameter (nm)

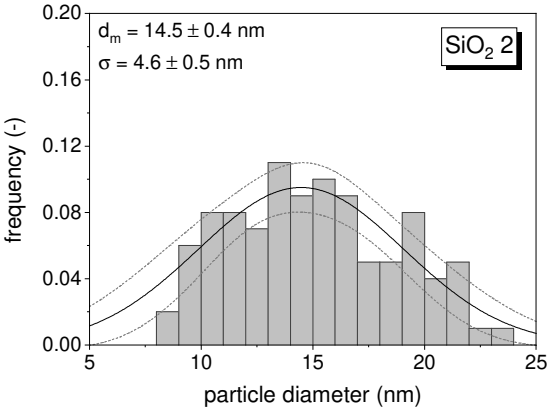
d_m = 14.5 ± 0.4 nm
σ = 4.6 ± 0.5 nm
SiO_2 2
frequency (-)
particle diameter (nm)

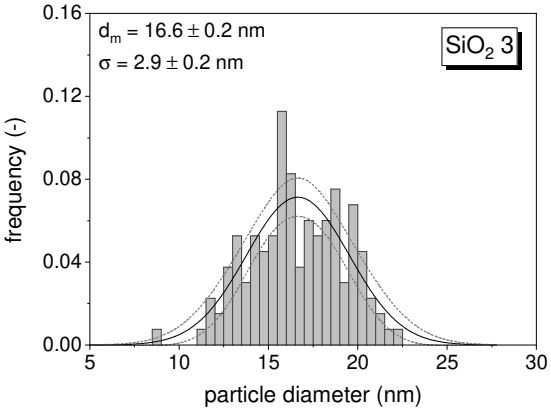
d_m = 16.6 ± 0.2 nm
σ = 2.9 ± 0.2 nm
SiO_2 3
frequency (-)
particle diameter (nm)

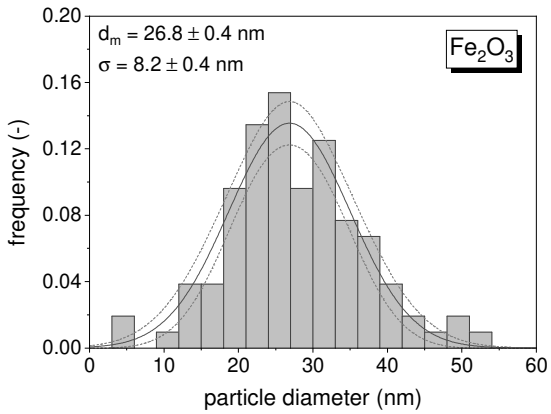
d_m = 26.8 ± 0.4 nm
σ = 8.2 ± 0.4 nm
Fe_2O_3
frequency (-)
particle diameter (nm)

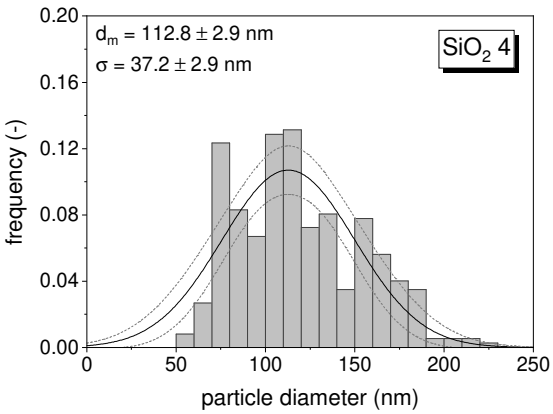
d_m = 112.8 ± 2.9 nm
σ = 37.2 ± 2.9 nm
SiO_2 4
frequency (-)
particle diameter (nm)

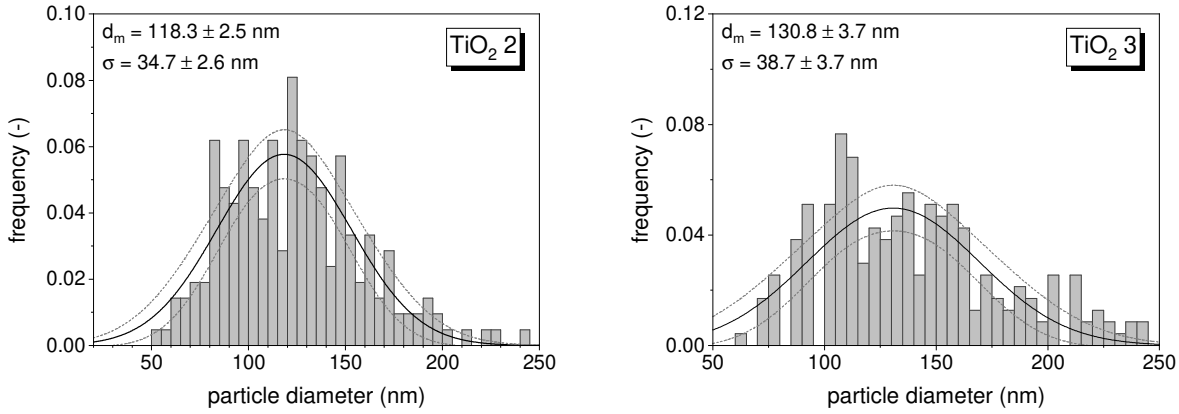

Figure 5. Number size distributions of constituent particles as determined by TEM image analysis according to equation 13. The solid lines correspond to fitted normal distributions, the dashed lines represent the associated 95% confidence interval.

VSSA-based constituent particle diameters

Data presented in Table 1 were used to determine the "raw" VSSA-based particle diameter $d_{VSSA,mono}$ according to equation 14. In parallel, number size distributions established from TEM picture analysis (Figure 5) were used as input parameters in the calculation of factor θ. Indeed, along with these number size distributions, Table 2 summarizes the ratio σ/d_m as well as the correlation coefficient associated with the normal fit. The latter θ values were used in the determination of $d_{VSSA,poly}$ as stated in equation 15.

Table 2. Characteristics of the constituent particle number size distributions presented in Figure 4 for the eight powders investigated.

Substance	$\frac{\sigma}{d_m}$ (-)	θ (-)	Normal fit correlation coefficient R^2 (-)
TiO_2 1	0.19	0.93	0.96
SiO_2 1	0.19	0.93	0.90
SiO_2 2	0.32	0.84	0.79
SiO_2 3	0.17	0.94	0.82
Fe_2O_3	0.30	0.86	0.93
SiO_2 4	0.33	0.84	0.83
TiO_2 2	0.29	0.86	0.79
TiO_2 3	0.30	0.86	0.65

It can be stated from Table 2 that the ratios σ/d_m observed for the eight powders under study range from 0.17 to 0.32. This leads to experimental values of θ between 0.94 and 0.84. The correlation coefficients reported in Table 2 are larger than 0.8 in most cases, which suggests that the selection of a normal distribution of the size of constituent particles is relevant for the powder samples considered here. It is noteworthy that other models could be used, insofar as they allow experimental data to be correctly fitted.

In spite of the limited amount of cases investigated, and as suggested earlier, the use of a polydispersion of $\sigma/d_m = 0.25$ is relevant regarding our experimental data. Indeed, Table 2 presents an average σ/d_m of 0.26. This assumed value of $\sigma/d_m = 0.25$, leading to $\theta = 0.9$, was used to determine $d^*_{VSSA,poly}$ (equation 15).

Comparison of the VSSA-based diameters to the TEM-based reference diameters

Figure 6 presents a comparison between the VSSA-based equivalent diameters for the different approaches: without accounting for constituent particle polydispersion ($d_{VSSA,mono}$), with polydispersion accounted, with either the experimental value ($d_{VSSA,poly}$) or the assumed value of $\sigma/d_m = 0.25$ ($d^*_{VSSA,poly}$) for the eight powders investigated.

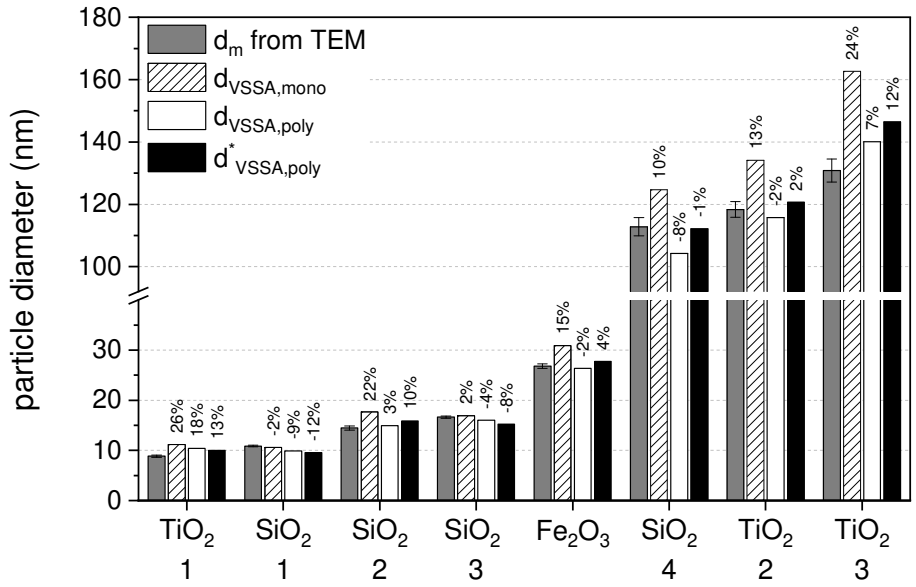

Figure 6. Comparison of particle diameters stemming from TEM image analysis (grey), VSSA approach without accounting for constituent particle polydispersion (white with black stripes) and VSSA approach with polydispersion accounted, with either the experimental value (white) or the assumed value of 0.25 (black) for the eight powders investigated. Values indicated on top of each bar correspond to the relative discrepancy between TEM-based and VSSA-based particle diameter.

From a general point of view, it can be observed in Figure 6 that accounting for constituent particles polydispersion results in a better agreement between the VSSA-based and the reference TEM-based diameters (d_m). This is valid for the whole range of median constituent particle diameter considered, which spans from 9 to 130 nm.

In the following, it was chosen to reason in terms of relative discrepancy, which is given by:

$$\Delta(\%) = 100\frac{d_{VSSA} - d_m}{d_m}$$

In Figure 6, the relative discrepancies are displayed on the top of each bar, with reference to the TEM-based median constituent particle size. In most cases, considering constituent particle polydispersion improves the resulting VSSA-based diameter, except for SiO_2 1 and 3. This might be due to the aggregated state of constituent particles, which makes it more difficult to determine their edges from TEM pictures, and therefore induces an uncertainty in the reference particle diameter.

More particularly, the relative discrepancies observed for $d_{VSSA,mono}$ range from -2% to 26%, while the ones related to $d_{VSSA,poly}$ are comprised between -9% and 18%. In addition, these discrepancies between $d_{VSSA,poly}$ and the reference were found independent from the correlation coefficient given in Table 2.

It is important to note that in the absence of the true value of σ/d_m, assuming a value of 0.25 as suggested, leads to corresponding particle diameters $d^*_{VSSA,poly}$ that are close to the reference TEM-based values. Indeed, the relative discrepancies range from -12% to 13%.

All these observations are summarized in Figure 7 as boxplots.

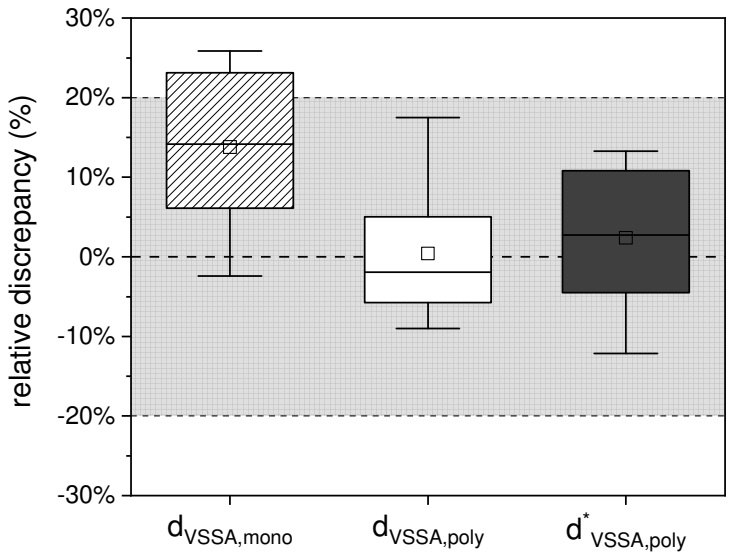

Figure 7. Boxplot (*n* = 8) representation of the relative discrepancies between TEM-based and VSSA-based equivalent diameter, for both monodisperse and the two polydisperse approaches.

It is clear from Figure 7 that accounting for constituent particle polydispersion improves the accurate determination of the median particle size. The approach considering constituent particles to be monodisperse leads to a majority (seven cases over the eight under study, that is to say 87%) of positive relative discrepancies, which means that this approach tends to overestimate particle size. This is perfectly in line with the fact that the $VSSA_{poly}$ of a powder consisting of polydisperse constituent particles is lower than the one of monodisperse particles with identical median diameter (see equations 10 and 14). In addition, in three cases among the eight considered, $d_{VSSA,mono}$ is found to be greater than the reference TEM-based d_m by more than 20%. On the contrary, both polydisperse approaches provide results that are within ± 20% from the reference diameter (grey area in Figure 7).

More precisely, the Inter-Quartile Ranges (IQR) of the relative discrepancies found for the three approaches investigated are [6% - 23%] for monodisperse particles, [-6% - 5%] for polydisperse particles with the "true" standard deviation considered, and [-5% – 11%] when polydispersion is supposed to be $\sigma/d_m = 0.25$. It is important to note that the narrowest IQR (50% confidence interval) is found for the polydisperse approach with experimental polydispersion considered. As represented by the squares in Figure 7, the mean relative discrepancies are 14%, 0% and 2%, for these three approaches, respectively. Interestingly, the alternative approach based on the assumption $\sigma/d_m = 0.25$ also leads to satisfactory results. Although limited in number (*n* = 8 materials considered) and restricted to spherical and normally-distributed constituent particles, the results presented here tend to suggest that it is useful to consider constituent particle polydispersion to improve the accuracy of particle size stemming from the $VSSA$ approach. In practice, this approach is promising and shall limit false-negative identification of nanomaterials without resorting to electron microscopy.

Conclusion and outlook

Volume Specific Surface-Area ($VSSA$) has been identified as a relevant and alternative method to electron microscopy to determine whether a material is or not a nanomaterial. Measuring the $VSSA$ of a material powder is readily accessible, since it relies on well disseminated measurement techniques in both research laboratories and industries. Contrary to electron microscopy, which is cost and time-consuming, measuring the $VSSA$ of a powder sample does not involve dispersion protocol, which reduces other possible artefacts. The

correct interpretation of gas adsorption data, and therefore the determination of the external surface area of the sample, is a key element of this alternative approach. In particular, care should be taken in the case of porous materials.

In practice, $VSSA$ can be used to determine particle diameter, named VSSA-based equivalent diameter, which can be further compared to the 100 nm threshold. However, this equivalent diameter depends on constituent particle polydispersion, since $VSSA$ involves integral measurement techniques. This issue has not been yet fully considered by authors who investigated the accuracy with which particle diameter can be derived from $VSSA$ measurements.

In this paper, the issue related to the effect of particle polydispersion on the $VSSA$ of a powder material was investigated. The specific case of normally-distributed, spherical non-porous constituent particles, has been considered, both theoretically and experimentally. Though this ideal case may not be universal, it could be further adapted to other situations, i.e. various particle shapes and size distribution laws.

First, the theoretical study has led to the introduction of a correction factor, noted θ, defined as a polydispersion-based coefficient. This coefficient depends on both the shape of the constituent particles and the mathematical function describing their size distribution.

Second, experimental data obtained for eight powders have been considered to determine the constituent particle median diameter stemming from $VSSA$ measurements, associated with TEM observations that allowed experimental factor θ to be calculated and integrated. In the absence of the experimental number size distribution of constituent particles, an alternative approach based on a hypothesis of constituent particle polydispersion was also studied. The latter constitutes a proposal that shall be further documented by implementing new data obtained for various samples.

The results provided by the three different approaches (VSSA-based diameters considering monodisperse particles, polydisperse particles with known or assumed polydispersion) were compared to the median constituent particle size obtained from electron microscopy analysis, considered as the reference method. The results demonstrate that considering constituent particle polydispersion improves the accuracy of particle size stemming from the $VSSA$ approach. For the eight materials investigated covering a range of constituent particle median diameters from 9 to 130 nm, the relative discrepancies were found within ± 20% from the reference diameter for both approaches accounting for polydispersion, the latter being either assumed or determined from TEM pictures. On the contrary, the relative discrepancies between VSSA-based and reference TEM constituent particle diameter was found beyond 20% in 3 cases out of 8 when particles are supposed to be monodisperse.

Further studies involving a larger number of materials are still necessary to make our findings more robust. The case of non-spherical particles shall also be investigated, e.g. the case of fiber-like or platelet-like particles. Indeed, particle shape directly affects the expression of the correction factor θ. In addition, the case of lognormally-distributed constituent particles, as well as bi- or multi-modal number size distributions, should be considered in future work.

Conflicts of interest

There are no conflicts to declare.

References

[1] EUROPEAN COMMISSION - Commission recommendation of 18 October 2011 on the definition of nanomaterial. *Off. J. Eur. Union*, 2011, **275,** 38.

[2] RAUSCHER H., MECH A., GIBSON N., GILLILAND D., HELD A., KESTENS V., KOEBER R., LINSINGER T., & STEFANIAK E. - Identification of nanomaterials through measurements. *Publications Office of the European Union*, 2019**,** doi: 10.2760/053982.

[3] MAVROCORDATOS D., PERRET D., & LEPPARD G. G. - Strategies and advances in the characterisation of environmental colloids by electron microscopy. *IUPAC SERIES ON ANALYTICAL AND PHYSICAL CHEMISTRY OF ENVIRONMENTAL SYSTEMS*, 2007, **10,** 345.

[4] BAU S., WITSCHGER O., GENSDARMES F., RASTOIX O., & THOMAS D. - A TEM-based method as an alternative to the BET method for measuring off-line the specific surface-area of nanoaerosols. *Powder Technology*, 2010, **200,** 190-201.

[5] FAVRE G., FELTIN N., & BAU S. - Mesure de la taille de nanoparticules : retour sur une comparaison inter-laboratoires et inter-techniques. *Hygiène et Sécurité du Travail*, 2020, **260,** 60-67.

[6] DAZON C., MAXIT B., & WITSCHGER O. - Comparison between a low-voltage benchtop electron microscope and conventional TEM for number size distribution of nearly spherical shape constituent particles of nanomaterial powders and colloids. *Micron*, 2019, **116,** 124-129.

[7] KREYLING W. G., SEMMLER-BEHNKEA M., & CHAUDHRYB Q. - A complementary definition of nanomaterials. *Nano Today*, 2010, **5,** 165-168.

[8] DAZON C., WITSCHGER O., BAU S., FIERRO V., & LLEWELLYN P. L. - Toward an operational methodology to identify industrial-scaled nanomaterial powders with the volume specific surface area criterion. *Nanoscale Advances*, 2019, **1,** 3232-3242.

[9] LECLOUX A. J. - Discussion about the use of the volume-specific surface area (VSSA) as criteria to identify nanomaterials according to the EU definition. *J. Nanopart. Res.*, 2015, **17,** 447.

[10] LECLOUX A. J., ATLURI R., KOLEN'KO Y. V., & DEEPAK F. L. - Discussion about the use of the volume specific surface area (VSSA) as a criterion to identify nanomaterials according to the EU definition. Part two: experimental approach. *Nanoscale*, 2017, **9,** 14952-14966.

[11] BABICK F., MIELKE J., WOHLLEBEN W., WEIGEL S., & HODOROABA V.-D. - How reliably can a material be classified as a nanomaterial? Available particle-sizing techniques at work. *J. Nanopart. Res.*, 2016, **18,** 158.

[12] SCENIHR - Scientific Basis for the Definition of the Term "nanomaterial" *http://ec.europa.eu/health/scientific_committees/emerging/docs/scenihr_o_032.pdf*, 2010.

[13] WOHLLEBEN W., MIELKE J., BIANCHIN A., GHANEM A., FREIBERGER H., RAUSCHER H., GEMEINERT M., & HODOROABA V.-D. - Reliable nanomaterial classification of powders using the volume-specific surface area method. *J. Nanopart. Res.*, 2017, **19,** 61.

[14] DAZON C., FIERRO V., CELZARD A., & WITSCHGER O. - Identification of nanomaterials by the volume specific surface area (VSSA) criterion: application to powder mixes. *Nanoscale Advances*, 2020, **2,** 4908-4917.

[15] MECH A., WOHLLEBEN W., GHANEM A., HODOROABA V. D., WEIGEL S., BABICK F., BRÜNGEL R., FRIEDRICH C. M., RASMUSSEN K., & RAUSCHER H. - Nano or Not Nano? A Structured Approach for Identifying Nanomaterials According to the European Commission's Definition. *Small*, 2020, **16,** 2002228.

[16] BRUNAUER S., EMMETT P. H., & TELLER E. - Adsorption of gases in multimolecular layers. *Journal of the American chemical society*, 1938, **60,** 309-319.

[17] LIPPENS B. C. & DE BOER J. - Studies on pore systems in catalysts: V. The t method. *Journal of Catalysis*, 1965, **4,** 319-323.

[18] MOTZKUS C., MACÉ T., GAIE-LEVREL F., DUCOURTIEUX S., DELVALLEE A., DIRSCHERL K., HODOROABA V.-D., POPOV I., POPOV O., KUSELMAN I., TAKAHATA K., EHARA K., AUSSET P., MAILLÉ M., MICHIELSEN N., BONDIGUEL S., GENSDARMES F., MORAWSKA L., JOHNSON G. R., FAGHIHI E. M., KIM C. S., KIM Y. H., CHU M. C., GUARDADO J. A., SALAS A., CAPANNELLI G., COSTA C., BOSTROM T., JÄMTING Å. K., LAWN M. A., ADLEM L., & VASLIN-REIMANN S. - Size characterization of airborne SiO2 nanoparticles with on-line and off-line measurement techniques: an interlaboratory comparison study. *J. Nanopart. Res.*, 2013, **15,** 1919.

[19] HACKLEY V. A. & STEFANIAK A. B. - "Real-world" precision, bias, and between-laboratory variation for surface area measurement of a titanium dioxide nanomaterial in powder form. *J. Nanopart. Res.*, 2013, **15,** 1742.

[20] ROEBUCK B. & MINGARD K. - WC powder characterisation: Technique intercomparison. *NPL REPORT MAT 32*, 2009**,** ISSN 1754-2987.

[21] THOMMES M., KANEKO K., NEIMARK A. V., OLIVIER J. P., RODRIGUEZ-REINOSO F., ROUQUEROL J., & SING K. S. W. - Physisorption of gases, with special reference to the evaluation of surface area and pore size distribution (IUPAC Technical Report). *Pure and Applied Chemistry*, 2015, **87,** 1051-1069.

[22] ROUQUEROL J., ROUQUEROL F., LLEWELLYN P., MAURIN G., & SING K. S. (2013) *Adsorption by powders and porous solids: principles, methodology and applications* (Academic press).

[23] WANG J., ASBACH C., FISSAN H., HÜLSER T., KUHLBUSCH T. A. J., THOMPSON D., & PUI D. Y. H. - How can nanobiotechnology oversight science and industry: examples from environmental, health, and safety studies of nanoparticles (nano-EHS). *J. Nanopart. Res.*, 2011, **13,** 1373-1387.

[24] BRODAY D. M. & ROSENZWEIG R. - Deposition of fractal-like soot aggregates in the human respiratory tract. *J. Aerosol Sci.*, 2011, **42,** 372-286.

[25] ICRP - *Publication 66: Human respiratory tract model for radiological protection*, 1994**,** Oxford: Pergamon.

[26] HINDS W. C. - Aerosol Technol. : Properties, Behavior, and Measurement of Airborne Particles. *John Wiley & Sons*, 1999.

[27] GAILLARD C., MECH A., WOHLLEBEN W., BABICK F., HODOROABA V.-D., GHANEM A., WEIGEL S., & RAUSCHER H. - A technique-driven materials categorisation scheme to support regulatory identification of nanomaterials. *Nanoscale Advances*, 2019, **1,** 781-791.

[28] POWERS K. W., PALAZUELOS M., MOUDGIL B. M., & ROBERTS S. M. - Characterization of the size, shape, and state of dispersion of nanoparticles for toxicological studies. *Nanotoxicology*, 2007, **1,** 42-51.

[29] DAZON C., WITSCHGER O., BAU S., FIERRO V., & LLEWELLYN P. L. - Nanomaterial identification of powders: comparing volume specific surface area, X-ray diffraction and scanning electron microscopy methods. *Environmental Science: Nano*, 2019, **6,** 152-162.

[30] AKBARI B., TAVANDASHTI M. P., & ZANDRAHIMI M. - Particle size characterization of nanoparticles–a practical approach. *Iranian Journal of Materials Science and Engineering*, 2011, **8,** 48-56.

[31] VIANA M., JOUANNIN P., PONTIER C., & CHULIA D. - About pycnometric density measurements. *Talanta*, 2002, **57,** 583-593.
[32] TAMARI S. - Optimum design of the constant-volume gas pycnometer for determining the volume of solid particles. *Measurement Science and Technology*, 2004, **15,** 549.
[33] RUDE T. J., STRAIT L. H., & RUHALA L. A. - Measurement of Fiber Density by Helium Pycnometry. *Journal of Composite Materials*, 2000, **34,** 1948-1958.
[34] BUSHELL G. & AMAL R. - Fractal Aggregates of Polydisperse Particles. *Journal of Colloid and Interface Science*, 1998, **205,** 459-469.
[35] CHARALAMPOPOULOS T. T. & SHU G. - Effects of polydispersity of chainlike aggregates on light-scattering properties and data inversion. *Appl. Opt.*, 2002, **41,** 723-733.
[36] LIU F., YANG M., HILL F. A., SNELLING D. R., & SMALLWOOD G. J. - Influence of polydisperse distributions of both primary particle and aggregate size on soot temperature in low-fluence LII. *Applied Physics B*, 2006, **83,** 383.
[37] FARIAS T. L., KÖYLÜ Ü. Ö., & CARVALHO M. G. - Effects of polydispersity of aggregates and primary particles on radiative properties of simulated soot. *Journal of Quantitative Spectroscopy and Radiative Transfer*, 1996, **55,** 357-371.
[38] YON J., LIU F., MORÁN J., & FUENTES A. - Impact of the primary particle polydispersity on the radiative properties of soot aggregates. *Proceedings of the Combustion Institute*, 2019, **37,** 1151-1159.
[39] DASTANPOUR R. & ROGAK S. N. - The effect of primary particle polydispersity on the morphology and mobility diameter of the fractal agglomerates in different flow regimes. *Journal of Aerosol Science*, 2016, **94,** 22-32.
[40] ENDO Y., CHEN D.-R., & PUI D. Y. H. - Effects of particle polydispersity and shape factor during dust cake loading on air filters. *Powder Technology*, 1998, **98,** 241-249.
[41] TRZASKUS K., ELSHOF M., KEMPERMAN A., & NIJMEIJER K. - Understanding the role of nanoparticle size and polydispersity in fouling development during dead-end microfiltration. *Journal of Membrane Science*, 2016, **516,** 152-161.
[42] ROEBBEN G., RAUSCHER H., AMENTA V., ASCHBERGER K., SANFELIU A. B., CALZOLAI L., EMONS H., GAILLARD C., GIBSON N., & HOLZWARTH U. (2014) (Part).
[43] RICE S. B., CHAN C., BROWN S. C., ESCHBACH P., HAN L., ENSOR D. S., STEFANIAK A. B., BONEVICH J., VLADÁR A. E., WALKER A. R. H., ZHENG J., STARNES C., STROMBERG A., YE J., & GRULKE E. A. - Particle size distributions by transmission electron microscopy: an interlaboratory comparison case study. *Metrologia*, 2013, **50,** 663-678.
[44] SÖDERLUND J., KISS L. B., NIKLASSON G. A., & GRANQVIST C. G. - Lognormal Size Distributions in Particle Growth Processes without Coagulation. *Physical Review Letters*, 1998, **80,** 2386-2388.
[45] GRANQVIST C. G. & BUHRMAN R. A. - Log-normal size distributions of ultrafine metal particles. *Solid State Communications*, 1976, **18,** 123-126.
[46] WEJRZANOWSKI T., PIELASZEK R., OPALIŃSKA A., MATYSIAK H., ŁOJKOWSKI W., & KURZYDŁOWSKI K. J. - Quantitative methods for nanopowders characterization. *Applied Surface Science*, 2006, **253,** 204-208.
[47] DE TEMMERMAN P.-J., LAMMERTYN J., DE KETELAERE B., KESTENS V., ROEBBEN G., VERLEYSEN E., & MAST J. - Measurement uncertainties of size, shape, and surface measurements using transmission electron microscopy of near-monodisperse, near-spherical nanoparticles. *J. Nanopart. Res.*, 2014, **16,** 2177.
[48] BOURROUS S., RIBEYRE Q., LINTIS L., YON J., BAU S., THOMAS D., VALLIÈRES C., & OUF F.-X. - A semi-automatic analysis tool for the determination of primary particle size, overlap coefficient and specific surface area of nanoparticles aggregates. *Journal of Aerosol Science*, 2018, **126,** 122-132.
[49] DE TEMMERMAN P.-J., VERLEYSEN E., LAMMERTYN J., & MAST J. - Semi-automatic size measurement of primary particles in aggregated nanomaterials by transmission electron microscopy. *Powder Technology*, 2014, **261,** 191-200.

[50] DE TEMMERMAN P.-J., VAN DOREN E., VERLEYSEN E., VAN DER STEDE Y., FRANCISCO M. A. D., & MAST J. - Quantitative characterization of agglomerates and aggregates of pyrogenic and precipitated amorphous silica nanomaterials by transmission electron microscopy. *Journal of nanobiotechnology*, 2012, **10,** 24.

[51] VERLEYSEN E., DE TEMMERMAN P.-J., VAN DOREN E., FRANCISCO M. A. D., & MAST J. - Quantitative characterization of aggregated and agglomerated titanium dioxide nanomaterials by transmission electron microscopy. *Powder technology*, 2014, **258,** 180-188.

[52] OLSON E. - The importance of sample preparation when measuring specific surface area. *Journal of GXP Compliance*, 2012, **16,** 52-62.

[53] SING K. S., ROUQUEROL F., & ROUQUEROL J. - Classical interpretation of physisorption isotherms at the gas-solid interface. *Adsorption by Powders and Porous Solids: Principles, Methodology and Applications*, 2013, **2,** 159-189.

[54] SING K. - The use of nitrogen adsorption for the characterisation of porous materials. *Colloids and Surfaces A: Physicochemical and Engineering Aspects*, 2001, **187-188,** 3-9.

Appendix: mathematical demonstration of equation 8

Starting from the definition of $VSSA_{poly}$ (equation 7), it can be written that:

$$VSSA_{poly} = \frac{\int_{d_{min}}^{d_{max}} \exp\left[-\frac{1}{2}\left(\frac{d-d_m}{\sigma}\right)^2\right] \pi d^2 \mathrm{d}d}{\int_{d_{min}}^{d_{max}} \exp\left[-\frac{1}{2}\left(\frac{d-d_m}{\sigma}\right)^2\right] \frac{\pi}{6} d^3 \mathrm{d}d} = 6\frac{I_1}{I_2} \qquad (A1)$$

Let us calculate each integral separately:

$$I_1 = \int_{d_{min}}^{d_{max}} \exp\left[-\frac{1}{2}\left(\frac{d-d_m}{\sigma}\right)^2\right] \pi d^2 \mathrm{d}d \qquad (A2)$$

$$I_2 = \int_{d_{min}}^{d_{max}} \exp\left[-\frac{1}{2}\left(\frac{d-d_m}{\sigma}\right)^2\right] \pi d^3 \mathrm{d}d \qquad (A3)$$

As the integration is performed over the whole range of diameters supposed to be normally distributed ($d_{min} = d_m - k.\sigma$ and $d_{max} = d_m + k.\sigma$), the following transformation of integration variable is operated:

$$x = \frac{d-d_m}{\sigma} \qquad (A4)$$

leading to these changes for the variable and the limits:

$$\mathrm{d}d = \sigma.\mathrm{d}x \qquad (A5)$$

$$x_{min} = -k \qquad (A6)$$

$$x_{max} = +k \qquad (A7)$$

Let us consider the case of I_1:

$$I_1 = \int_{-k}^{k} \sigma.\exp\left(-\frac{x^2}{2}\right)(\sigma x + d_m)^2 \mathrm{d}x \qquad (A8)$$

$$I_1 = \sigma \int_{-k}^{k} \exp\left(-\frac{x^2}{2}\right)(\sigma^2 x^2 + 2\sigma x d_m + d_m^2)\mathrm{d}x \qquad (A9)$$

$$I_1 = \sigma\left[\int_{-k}^{k} \exp\left(-\frac{x^2}{2}\right)\sigma^2 x^2 \mathrm{d}x + \int_{-k}^{k} \exp\left(-\frac{x^2}{2}\right)2\sigma x d_m \mathrm{d}x + \int_{-k}^{k} \exp\left(-\frac{x^2}{2}\right) d_m^2 \mathrm{d}x\right] \qquad (A10)$$

Due to the parity properties of the functions in this expanded expression of I_1, equation A10 can be simplified as:

$$I_1 = \sigma\left[2\sigma^2 \int_{0}^{k} \exp\left(-\frac{x^2}{2}\right)(x^2)\mathrm{d}x + 2d_m^2 \int_{0}^{k} \exp\left(-\frac{x^2}{2}\right)\mathrm{d}x\right] \qquad (A11)$$

Considering the remaining terms in I_1:

$$I_1 = \sigma[I_{11} + I_{12}] \qquad (A12)$$

Because:

$$\int_{0}^{k} \exp\left(-\frac{x^2}{2}\right)\mathrm{d}x = \sqrt{\frac{\pi}{2}}\,\mathrm{erf}\left(\frac{k}{\sqrt{2}}\right) \qquad (A13)$$

the following calculations can be performed:

$$I_{12} = 2d_m^2 \int_{0}^{k} \exp\left(-\frac{1}{2}x^2\right)\mathrm{d}x = 2d_m^2\sqrt{\frac{\pi}{2}}\,\mathrm{erf}\left(\frac{k}{\sqrt{2}}\right) \qquad (A14)$$

As for I_{11}, a suitable integration by parts with equations A15 and A16 leads to relation A17:

$$u' = x.\exp\left(-\frac{x^2}{2}\right) \qquad (A15)$$

$$v = x \qquad (A16)$$

$$\begin{aligned}\int_{0}^{k} \exp\left(-\frac{x^2}{2}\right)x^2\mathrm{d}x &= \left[-x.\exp\left(-\frac{x^2}{2}\right)\right]_0^k + \sqrt{\frac{\pi}{2}}\,\mathrm{erf}\left(\frac{k}{\sqrt{2}}\right) \\ &= -k.\exp\left(-\frac{k^2}{2}\right) + \sqrt{\frac{\pi}{2}}\,\mathrm{erf}\left(\frac{k}{\sqrt{2}}\right)\end{aligned} \qquad (A17)$$

As the integration is processed over the whole range of diameters ($k = 5$), it can be reasonably assumed that:

$$k.\exp\left(-\frac{k^2}{2}\right) \approx 0 \qquad (A18)$$

and that:

$$\mathrm{erf}\left(\frac{k}{\sqrt{2}}\right) = 1 \qquad (A19)$$

Finally, this yields:

$$I_{11} = 2\sigma^2\sqrt{\frac{\pi}{2}} \qquad (A20)$$

And therefore:

$$I_1 = \sigma\sqrt{2\pi}(\sigma^2 + d_m^2) \tag{A21}$$

The second integral I_2can be evaluated in a similar manner:

$$I_2 = \sigma \int_{-k}^{k} \exp\left(-\frac{x^2}{2}\right)(\sigma^3 x^3 + 3\sigma^2 x^2 d_m + 3\sigma x d_m^2 + d_m^3)\mathrm{d}x \tag{A22}$$

$$I_2 = \sigma\left[6\sigma^2 d_m \int_{0}^{k} \exp\left(-\frac{x^2}{2}\right)(x^2)\mathrm{d}x + 2d_m^3 \int_{0}^{k} \exp\left(-\frac{x^2}{2}\right)\mathrm{d}x\right] \tag{A23}$$

Using equations A13, A18 and A19 yields:

$$I_2 = \sigma\left[6\sigma^2 d_m\sqrt{\frac{\pi}{2}} + 2d_m^3\sqrt{\frac{\pi}{2}}\right] = \sigma\sqrt{2\pi}(d_m^3 + 3\sigma^2 d_m) \tag{A24}$$

Thus, gathering the results obtained for I_1 and I_2 leads to:

$$\begin{aligned} VSSA_{poly} &= 6\frac{I_1}{I_2} \\ &= 6\frac{\sigma\sqrt{2\pi}(\sigma^2 + d_m^2)}{\sigma\sqrt{2\pi}(d_m^3 + 3\sigma^2 d_m)} \\ &= 6\frac{d_m^2\left(\frac{\sigma^2}{d_m^2} + 1\right)}{d_m^3\left(1 + 3\frac{\sigma^2}{d_m^2}\right)} \end{aligned}$$

which corresponds to equation 8 in the manuscript:

$$VSSA_{poly} = \frac{6}{d_m}\frac{1 + \left(\frac{\sigma}{d_m}\right)^2}{1 + 3\left(\frac{\sigma}{d_m}\right)^2}$$

Graphical abstract